Electron transport in metal oxide superconducting heterojunctions

F. V. Komissinski

Institute of Radio Engineering and Electronics, Russian Academy of Sciences, Moscow 125009, Russia; Department of Microtechnology and Nanoscience, Chalmers University of Technology, Göteborg S412 96, Sweden*

K. I. Constantinian, Yu. Kislinskii, and G. A. Ovsyannikov

Institute of Radio Engineering and Electronics, Russian Academy of Sciences, Moscow 125009, Russia

(Submitted January 23, 2004)
Fiz. Nizk. Temp. **30**, 795–809 (July–August 2004)

Research results on electron transport in $Au/YBa_2Cu_3O_x$ and $Nb/Au/YBa_2Cu_3O_x$ thin-film heterojunctions are reviewed. The experimental current–phase relations of $Nb/Au/YBa_2Cu_3O_x$ heterojunctions on *c*-oriented YBCO films exhibit a second harmonic, temperature dependence, and a phase shift that is explained in terms of a combined symmetry $d_{x^2-y^2}+s$ of the superconducting order parameter of $YBa_2Cu_3O_x$. The current–voltage characteristics of $Au/YBa_2Cu_3O_x$ and $Nb/Au/YBa_2Cu_3O_x$ heterojunctions on $(1\,1\,20)YBa_2Cu_3O_x$ thin films with an inclined crystallographic *c* axis display an anomaly of the conductance at low voltages, the behavior of which is studied at various temperatures and magnetic fields. The experimental results are analyzed in the framework of a model for the appearance of bound states caused by multiple Andreev reflection in junctions containing a superconductor with $d_{x^2-y^2}$ symmetry of the superconducting order parameter. Studies of the noise characteristics of $Nb/Au/(1\,1\,20)YBa_2Cu_3O_x$ heterojunctions at $T=4.2$ K reveal the presence of thermal and shot components. However, enhancement of the shot noise due to multiple Andreev reflection is not observed in the experiment. © *2004 American Institute of Physics.*
[DOI: 10.1063/1.1789918]

1. INTRODUCTION

The results of various experiments indicate that in the majority of metal oxide superconductors a complex type of symmetry of the superconducting order parameter is realized, in which the $d_{x^2-y^2}$ component is dominant (*d*-superconductors).[1] Unlike superconductors with isotropic (having *s* symmetry) superconducting order parameters (*s*-superconductors), in *d*-superconductors the order parameter changes sign upon a 90° change in direction of the quasiparticle momentum in the *ab* plane. As a consequence, in Josephson junctions based on *d*-superconductors, when a transport current is flowing in the *ab* plane in a direction for which the magnitude of the superconducting order parameter equals zero, the shape of the current–phase relation (CPR) can differ from sinusoidal.[2] A nonsinusoidal CPR, containing components proportional to $\sin\varphi$ and $\sin 2\varphi$, has been observed in experiments[3] in symmetric 45° bicrystal Josephson junctions with a [001]-inclined bicrystal boundary.

A different situation is realized in d/s heterojunctions (the slash/denotes a potential barrier) for the direction perpendicular to the *ab* basal plane (along the crystallographic *c* axis). Because of the *d* symmetry of the order parameter, the superconducting current in such heterojunctions should be small (proportional to the second power of the boundary transparency $\overline{D^2}$) and should contain a $\sin 2\varphi$ component corresponding to the second harmonic of the CPR.[2] However, the experimentally observed[4–6] product of the critical current J_c times the normal resistance R_N of the Josephson junction depends weakly on the boundary transparency, but it decreases if an epitaxial film having twin boundaries is used instead of a single crystal.[5] The experimental data can be explained by assuming that in thin films both types of symmetry of the superconducting order parameter (*s* and *d*) are realized and that a change in sign of the *s* component (a change of its phase by π) occurs at a twin boundary, while the *d* component remains unchanged.[6] Studies of the CPR of $Pb/YBa_2Cu_3O_x$ junctions on *c*-oriented $YBa_2Cu_3O_x$ films (*c*-YBCO) from the appearance of fractional Shapiro steps under irradiation by millimeter waves have shown the absence of a second harmonic of the CPR.[5]

In tunnel junctions of a *d*-superconductor with a normal metal (N/d), with an *s*-superconductor (s/d), or with another *d*-superconductor (d/d') the change in sign of the superconducting order parameter of the *d*-superconductor for the incident and Andreev-reflected quasiparticle gives rise to an additional phase shift by π.[7] Such a process is realized, for example, in N/d junctions with a (110)-oriented *d*-superconductor. The sequence of specular and Andreev reflections of a quasiparticle in this case causes Andreev bound states to form at low energies on the (110) plane of a *d*-superconductor, localized near the interface[1)] at a distance of the order of the coherence length.[8] Low-energy Andreev bound states (LABSs) are manifested in the appearance of a conductance peak at zero bias (conductance anomaly) on the current–voltage (I–V) characteristic of an N/d junction.[9]

Tunneling spectroscopy of metal oxide superconductors, YBCO in particular, is difficult because of the short coherence length of the material (≈ 3 nm) and also the high sen-

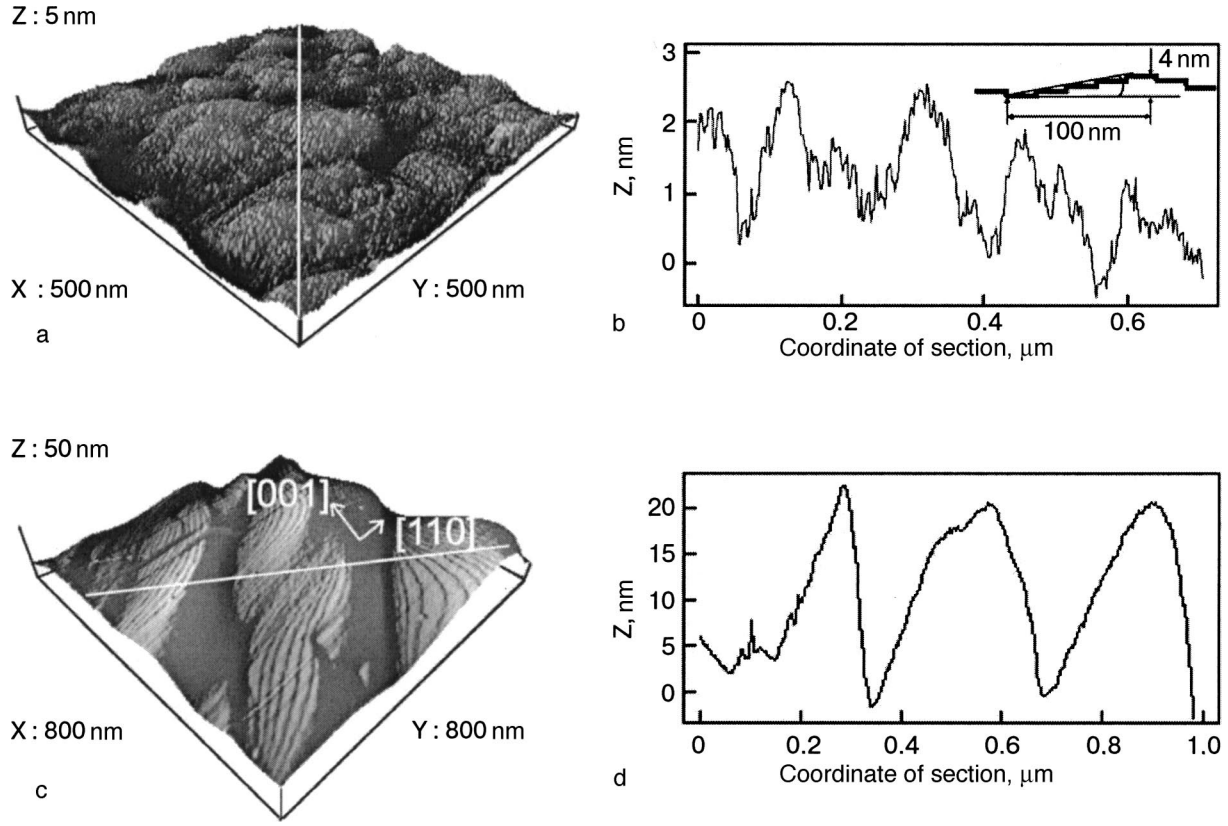

FIG. 1. Image of a portion of the surface, obtained with an atomic force microscope: *c*-oriented (*a*) and (1 1 20)-oriented (*c*) YBCO films. Profiles of the surface of the *c*-oriented (*b*) and (1 1 20)-oriented (*d*) YBCO films along the white lines in (*a*) and (*c*), respectively; the inset to panel *b* shows a schematic illustration of the structure of the surface of the *c*-oriented films.

sitivity to defects of the crystal lattice and to the presence of impurities. At the same time, as the experiment of Ref. 9 showed, the conductance anomaly has been observed in N/d and s/d heterojunctions, bicrystal junctions, end heterojunctions, and the point contacts of a scanning tunneling microscope. Therefore, of the two possible causes for the onset of the conductance anomaly, viz., the presence of magnetic impurities in the barrier[9] and LABSs in a *d*-superconductor,[8] a preference must be given to the latter. Theoretical studies have predicted the existence of LABSs on crystallographic planes of *d*-superconductors differing slightly from (110),[10] for example, on ''faceted'' surfaces,[11] and that prediction has been confirmed in experiments.[12] The experimentally observed splitting of the LABSs at high magnetic fields[12] was explained by a Doppler shift of the levels, caused by the flow of the screening current—the excitation of an imaginary *s* component of the superconducting order parameter in a surface layer of a *d*-superconductor.[12]

In this paper we review the results of experimental research on Au/YBCO and Nb/Au/YBCO heterojunctions based on *c*-oriented YBCO films on (001)$SrTiO_3$ substrates (*c* heterojunctions, *c*-HJs) and also single-domain films of (1 1 20)YBCO, which were prepared on specially oriented (7 10 2)$NdGaO_3$ substrates (inclined heterojunctions, IHJs).[13] We study the I–V characteristics of heterojunctions at low temperatures and low magnetic fields and also under irradiation by monochromatic millimeter-wave radiation. We analyze the current–phase relations of Nb/Au/YBCO heterojunctions of both types, obtained by the methods of rf superconducting quantum interference (SQUID)[14] and Shapiro steps.[15] We present the temperature dependence and magnetic-field dependence of the observed conductance anomaly on the I–V characteristic of the IHJ. In the Nb/Au/(1 1 20)YBCO IHJ at low temperatures we measured the noise characteristics and revealed the presence of thermal and shot components. The experimental results are discussed in the framework of a model for the onset of bound states due to Andreev reflection in superconductors with *d*-type symmetry of the superconducting order parameter.

2. PREPARATION OF THE HETEROJUNCTIONS AND THE MEASUREMENT TECHNIQUES

The *c*-oriented YBCO superconducting films were grown on (001)$SrTiO_3$ substrates. The *c* axis of the YBCO films grown on (7 10 2)NGO deviated from the normal to the plane of the substrate by an angle $\alpha \approx 11°$ of rotation in the (110)YBCO plane. As a result, the orientation of the YBCO film was close to (1 1 20)YBCO. YBCO epitaxial films 150 nm thick were laser deposited at a temperature of 770–790 °C in an oxygen atmosphere with a pressure of 0.6 mbar. The resulting YBCO films had a critical temperature $T_c = 85–90$ K and a critical current density $J_c \approx 2 \times 10^6$ and 5×10^4 A/cm^2 at 77 K for the *c*- and (1 1 20)-oriented YBCO films, respectively.[2)]

The morphology of our YBCO films was studied on an atomic force microscope. For the *c*-oriented YBCO films ($\alpha = 0$) the maximum surface roughness was 3–4 nm (Fig. 1*a*,*b*). With increasing angle α, growth steps appear on the surface, and at $\alpha = 11°$ [for (1 1 20)YBCO] their height is 20

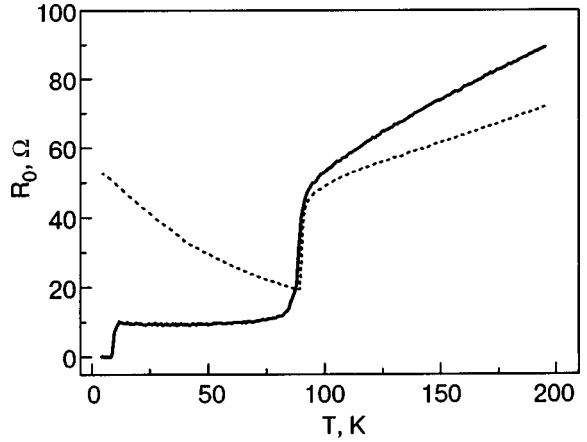

FIG. 2. Temperature dependence of the zero-bias resistance $R_0(T)$ for c-HJs Au/YBCO (dotted curve) and a Nb/Au/YBCO (solid curve) measured at a bias current of 1 μA.

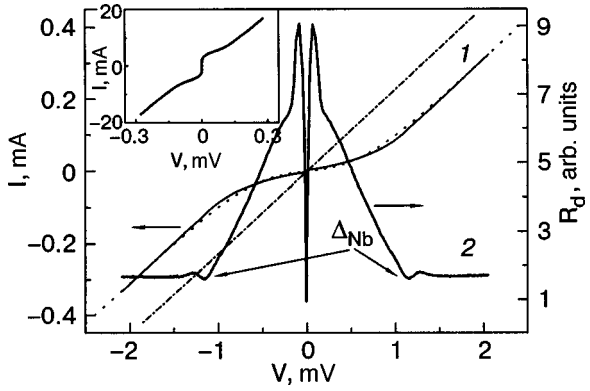

FIG. 3. I–V characteristic (*1*) and the voltage dependence of the differential resistance $R_d(V)$ of a Nb/Au/YBCO c-HJ at $T=4.2$ K (*2*). The dotted curve shows the dependence that follows from formula (1); the dot-and-dash line is Ohm's law $V=IR_N$. The inset shows the I–V characteristic in the range of voltages $V<0.3$ mV.

nm (Fig. 1*c*,*d*). The long and short sides of the growth steps are the (001) and (110) planes of YBCO, respectively. Therefore, in planar heterojunctions prepared on such YBCO films the total transport current is made up of the currents flowing through the contacts to the (001) and (110) crystallographic planes of YBCO. Because of the anisotropy of the conductivity of YBCO, a large part of the current flows through the (110)-oriented faces of the surface of the YBCO film.[16] We note that the surface roughness of (120)YBCO films on the (001)- and (110)-oriented faces is 1–2 lattice constants of the YBCO film.

For the formation of heterojunctions with areas A ranging from 5×5 to 30×30 μm we use the method of rf magnetron sputtering of Au and Nb, photolithography, and ion-beam etching in an argon atmosphere.[17] The eletrophysical parameters of the heterojunctions were measured in a four-point scheme in the fixed-current regime in the temperature range $T=4.2-300$ K, at magnetic fields up to 5 T, and under electromagnetic irradiation at frequencies of 40–100 GHz. The noise properties of the Nb/Au/(1 1 20)YBCO heterojunctions were investigated by two methods: direct measurement of the noise spectral density with a low-noise cooled amplifier working in the frequency range 1–2 GHz, and by the method of estimating the linewidth of the characteristic Josephson generation from the selective detector response to a weak external microwave signal.

3. HETEROJUNCTIONS ON *c*-ORIENTED YBCO FILMS AND THEIR PROPERTIES

3.1. Temperature dependence of the conductance of *c* heterojunctions

Figure 2 shows the temperature dependence of the resistance $R_0(T)$ at a low bias current (1 μA) for Au/YBCO and Nb/Au/YBCO c-HJs. At $T>T_c$ the resistance R_e of the YBCO leads is much larger than the resistance of the c-HJs, and therefore in this temperature region $R_0(T)$ characterizes the conductance of the leads in the ab basal plane of YBCO. It is seen in Fig. 2 that both curves correspond to a metallic type of conduction—the values of R_0 decrease with decreasing temperature. The value $T_c=84$ K of the YBCO leads for the Nb/Au/YBCO c-HJ is considerably lower than the analogous value $T_c=89.5$ K for the Au/YBCO c-HJ, probably because of the large number of technological operations in the fabrication of the Nb/Au/YBCO c-HJ and the resulting oxygen deficit in the surface layer of the YBCO film. At $T<T_c$ the behavior of $R_0(T)$ is fundamentally changed. For the Au/YBCO c-HJ at $T<T_c$ one observes the characteristic growth of R_0 for superconductor–insulator–normal metal tunnel junctions, while for the Nb/Au/YBCO c-HJ the resistance $R_0(T)\approx$const and remains unchanged down to the temperature of the transition of the niobium electrode to the superconducting state, $T_{cNb}\approx9.1$ K. Such behavior of $R(T)$ for the Nb/Au/YBCO c-HJ is apparently due to the presence in these c-HJs of a second interface, with a high transparency, between Nb and Au: in this regard the Au/Nb/YBCO c-HJ can be regarded as a highly asymmetric double-barrier structure $N/N'/s$, the conductance of which has a linear temperature dependence.[18]

3.2. I–V characteristics of Nb/Au/YBCO *c*-HJs

The I–V characteristics and the voltage dependence of the differential resistance $R_d(V)$ of the junction are shown in Fig. 3. The I–V characteristic of the c-HJ reveals the existence of a supercurrent with $J_c=1-10$ A/cm^2 and $I_cR_N=10-80$ μV in the c-HJ samples studied. Here R_N is the normal resistance of the junction, which is determined from the value of the differential resistance R_d of the junction at voltages $V\geqslant2$ mV. We also note that at $V>2$ mV the $R_d(V)$ curve is descending with increasing voltage, like that of the Au/YBCO c-HJ. The descending trend of $R_d(V)$ persists even at $V>\Delta_d=20$ mV, the value obtained in tunneling microscope experiments.[19]

At low voltages the I–V characteristic of the junction corresponds well to a resistive model of the Josephson junction, with low capacitance (see the inset in Fig. 3). When the voltage is increased to $V>2$ mV the I–V characteristic has the form $V=(I+I_e)R_N$, where $I_e<0$ is the excess current. $I_e>0$ is observed in superconducting junctions with direct (not tunneling) conduction.[20,21] Negative I_e (a current deficit) is typical of double-barrier superconducting heterostructures $s/N/s'$, in which with decreasing proximity effect in the N layer a change in sign of I_e is observed (a transition from a

current excess to a current deficit).[20] As we see in Fig. 3, the I–V characteristic of the junctions is well described by the relation typical for $s/N/s'$ structures:[22]

$$V = IR_N + I_e R_N \tanh(eV/kT). \quad (1)$$

From the experimentally measured I–V characteristic for this junction we have $I_e = -145$ μA at $T = 4.2$ K. According to Ref. 22, $I_e = (-\overline{D}\Delta_d - \Delta_{\rm Nb})/(eR_N) \approx -270$ μA, where $\Delta_{\rm Nb} = 1.2$ mV is the superconducting gap of Nb, and $\overline{D} \approx 7.6 \times 10^{-5}$ is the transparency, averaged over the area of the junction, of the Au/YBCO boundary, calculated according to the formula[20–22]

$$\overline{D} = 2\rho l/3r, \quad (2)$$

where $r = R_N A = 4.4 \times 10^{-6}$ $\Omega \cdot \text{cm}^2$ is the characteristic resistance of the contact ($R_N \equiv R_0(T_c)$), and $\rho = \rho_c \sim 5 \times 10^{-3}$ $\Omega \cdot$cm and $l = l_c \approx 1$ nm are, respectively, the resistivity and mean free path in the superconductor, the latter being equal to the distance between CuO_2 planes in the YBCO film (Ref. 16).[3)]

The $R_d(V)$ curve exhibits a feature in the form a local minimum at $V = 1.2$ mV, which coincides in value with $\Delta_{\rm Nb}$ and has a temperature dependence close to that given by BCS theory. This feature on the I–V characteristic vanishes together with the critical current at $T = 8.5$–9.1 K, and the temperature dependence of $I_c(T)$ is close to that of $\Delta_{\rm Nb}(T)$. We note that previously the gap structure of the *s*-superconductor Pb was observed in a Pb/YBCO *c*-HJ.[4]

To estimate the contribution to the measured resistance from the electron transport caused by the contact to the *ab* basal plane of the YBCO film, we used a parallel-resistor model for the resistances of the sharp boundaries between Au and YBCO along the *c* axis (r_c) and in the basal plane of YBCO (r_{ab}). Here r for the heterojunctions was determined from the condition

$$r = r_c r_{ab}/(r_{ab} + r_c \tan\gamma), \quad (3)$$

where $\tan\gamma \approx A_{ab}/A \approx 0.04$ and A_{ab} is the total area of the contacts to the *ab* plane of the YBCO film (see the inset to Fig. 1*b*). In Refs. 17 and 23 it was shown that for YBCO the experimentally observed values of r_c are an order of magnitude larger than r_{ab}. Consequently, for surface irregularities observed in experiment ($\gamma \approx 2°$), the contribution to the total current from the component of the contacts to the *ab* planes is small. This is confirmed by the absence of a conductance peak at low voltages—the conductance anomaly due to Andreev reflection in the *d*-superconductor—for the Nb/Au/YBCO junctions at $T > T_{c\rm Nb}$ (see also Sec. 4 of the present paper).[8] We recall that the theory predicts the appearance of such an anomaly for rough boundaries of N/d heterojunctions even in the case of an arbitrarily oriented *d*-superconductor.[11]

We note that superconducting shorts do not form in regions of possible punchthrough of the Au film (e.g., nonstoichiometric particles on the surface of the YBCO film). In particular, studies of Nb contacts to YBCO without the Au spacer layer on specially prepared samples revealed the absence of supercurrent and $r_c \sim 1$ $\Omega \cdot \text{cm}^2$, which is apparently a consequence of the active chemical interaction of Nb with oxygen from the YBCO film, with the formation of Nb_2O_5 and other oxides of Nb (see also Ref. 24).

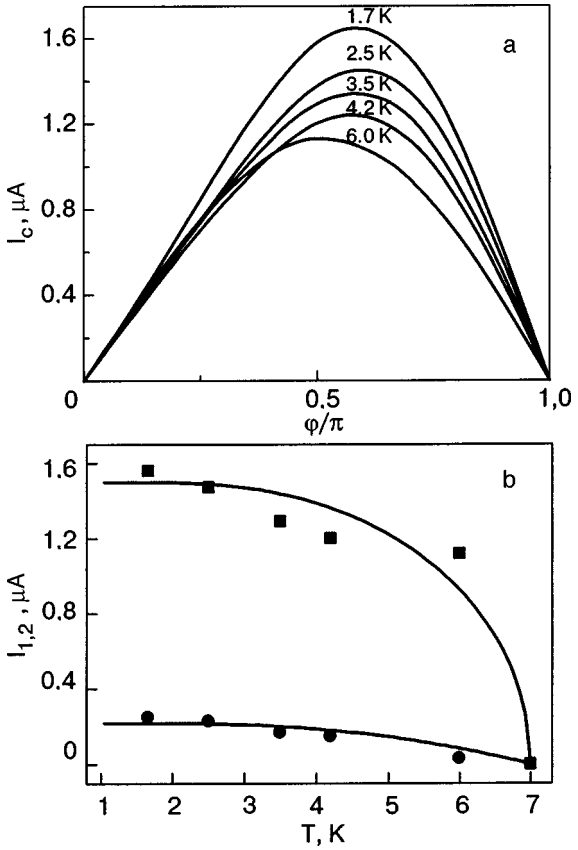

FIG. 4. Current–phase relation for a Nb/Au/YBCO *c*-HJ at temperatures of 1.7, 2.5, 3.5, 4.2, and 6.0 K (*a*). Temperature dependence of $I_1(T)$ (squares) and $I_2(T)$ (circles). The solid lines show the theoretical curves of $I_1(T)$ and $I_2(T)$ calculated according to formulas (6) and (7) (*b*).

3.3. Phase dependence of the supercurrent of a Nb/Au/YBCO *c*-HJ

For measurement of the dependence of the supercurrent on the phase different of the wave functions, $I_s(\varphi)$, we used a method in which a Nb/Au/YBCO *c*-HJ with dimensions of 10×10 μm was shorted by a ring of YBCO film with an inductance $L \approx 80$ pH and by another Nb/Au/YBCO *c*-HJ with a substantially larger area of 100×100 μm, forming a SQUID. The current–phase relation was calculated from the measurements of the amplitude–frequency characteristics of an rf resonator inductively coupled with this SQUID. This method is differential with respect to φ and gives high sensitivity in measurements of current–phase relations.[14]

In the temperature range $T = 1.7$–6.0 K in which the CPR was measured, the normalized critical current $\beta_L = 2\pi L I_c/\Phi_0$ ($\Phi_0 = 2.07 \times 10^{-15}$ Wb is the magnetic flux quantum) of the Nb/Au/YBCO *c*-HJ under study lay in the interval from 0.27 to 0.4, i.e., $\beta_L < 1$. Therefore the CPR could be determined for a whole period of variation of φ.[14] The CPR of a Nb/Au/YBCO *c*-HJ is shown in Fig. 4. It is seen that with decreasing temperature the shape of the current–phase relation begins to deviate from sinusoidal. A Fourier analysis of the measured CPR showed that its spectrum contains a finite number of first and second harmonics

and that the amplitudes of higher-order harmonics are small. Therefore, the superconducting component of the current can be written in the form

$$I_s(\varphi)=I_{c1}\sin\varphi+I_{c2}\sin(2\varphi+\varphi_0). \tag{4}$$

The experimentally observed sign of the I_{c2} term is always opposite to that of the I_{c1} term, i.e., $\varphi_0=\pi$. If $T\approx 1.7$ K, then $I_{c1}=1.57\ \mu$A, $I_{c2}=-0.25\ \mu$A, and $|I_{c2}/I_{c1}|\approx 0.16$. The temperature dependence of $I_{c1}(T)$ and $I_{c2}(T)$ is shown in Fig. 4*b*.[25]

After completion of the measurements of the CPRs the YBCO superconducting inductive ring of the SQUID was locally cut by a focused ion beam. In the resulting geometry we then measured the I–V characteristic and the $R_d(V)$ curve of the same Nb/Au/YBCO *c*-HJ for which the CPR had been measured. From the $R_d(V)$ curve we determined the value $R_N\approx 60\ \Omega$, which corresponds to $r_c=6\times10^{-5}\ \Omega\cdot\text{cm}^2$, and then, using Eq. (2), obtained the transparency of the given *c*-HJ: $\overline{D}\approx 5.6\times10^{-5}$.

The CPR of the *c*-HJ was also measured by a different method, based on measurement of the critical current and of the Shapiro steps on the I–V characteristic of a Nb/Au/YBCO *c*-HJ as functions of the amplitude of an external monochromatic electromagnetic wave irradiating the heterojunction.[15,26] Under external monochromatic electromagnetic irradiation at frequency $f_e\approx 40$ GHz Shapiro steps I_n corresponding to the fundamental frequency and a harmonic component appeared on the I–V characteristic at voltages of $n(hf/2e)$ (n is an integer). At a voltage of $\frac{1}{2}(hf/2e)$ ($n=1/2$) the first subharmonic Shapiro step was also observed, with an amplitude $I_{1/2}/I_c=0.08$ at $T=4.2$ K. Figure 5 shows I_c, I_1, and $I_{1/2}$ as functions of the amplitude of the rf current. The solid curves show the theoretical dependences $I_c(a)$, $I_1(a)$, and $I_{1/2}(a)$, where $a=I_{RF}/I_c$ is the experimental value of the normalized rf current, which was determined from a comparison of the experimental $I_1(a)$ curve with the theoretical one in respect to the first minimum of this quantity.[15] We note that for low amplitudes of the external radiation the first Shapiro step is symmetric with respect to the autonomous I–V characteristic, a circumstance that attests to the coherence of the Josephson generation in autonomous junctions.[26] Thus the subharmonic Shapiro steps observed on the experimental I–V characteristic may be indicative of a deviation of the dependence $I_s(\varphi)$ from sinusoidal. At $T=4.2$ K the ratios of the harmonics of the CPR determined by the rf SQUID method and also from the amplitudes of the Shapiro steps are $|I_{c2}/I_{c1}|\approx 0.12$ and $I_{1/2}/I_c=0.08$ for two *c*-HJs on one substrate.

The presence of the two harmonics $I_{c1}\propto\sin\varphi$ and $I_{c2}\propto\sin 2\varphi$ in the spectrum of the CPR of a Nb/Au/YBCO *c*-HJ can be explained by the existence of a combined $d+s$ symmetry of the superconducting order parameter in YBCO. For calculation of the supercurrent we use the expression[25]

$$I_s(\varphi)=\frac{2e}{\hbar}\sum_{k,\theta}k_BT\sum_{\omega}\times\frac{D(\theta)\Delta_R\Delta_k\sin\varphi}{2\Omega_R\Omega_k+D(\theta)(\omega^2+\Omega_R\Omega_k+\Delta_R\Delta_k\cos\varphi)}. \tag{5}$$

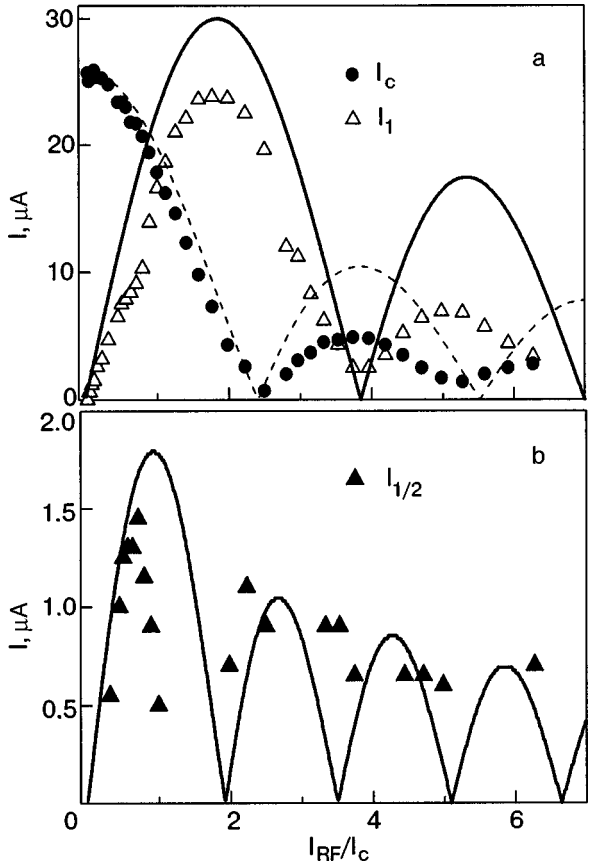

FIG. 5. Critical current I_c and the first Shapiro step I_1 (*a*) and the first subharmonic Shapiro step $I_{1/2}$ (*b*) on the experimental I–V characteristic of a Nb/Au/YBCO *c*-HJ as functions of the amplitude of 40-GHz electromagnetic radiation, normalized to I_c, at $T=4.2$ K. The solid and dashed curves show the corresponding dependences that follow from a resistive model of the Josephson junctions.

In formula (5) Δ_R and Δ_k denote the superconducting gaps of Nb and YBCO, respectively, and $\Omega_{R,k}=\sqrt{\omega^2+\Delta_{R,k}^2}$. Keeping in Eq. (5) terms up to second order in the small quantity $D(\theta)\ll 1$ inclusive, we obtain[25]

$$I_{c1}(T)R_N\approx\frac{\Delta_s}{\Delta_d^*}\frac{\Delta_R(T)}{e}, \tag{6}$$

$$I_{c2}(T)R_N\approx-\frac{\pi}{8}\overline{D}\frac{\Delta_R(T)}{e}\tanh\left(\frac{\Delta_R(T)}{2k_BT}\right), \tag{7}$$

where $\Delta_d^*=\pi\Delta_d[2\ln(3.56\Delta_d/k_BT_{cR})]^{-1}$. In deriving formulas (6) and (7) we have used an expression for the superconducting gap of YBCO of the form $\Delta(\theta)=\Delta_d\cos 2\theta+\Delta_s$, where Δ_d and Δ_s are the amplitude values of the *d* and *s* components of the superconducting order parameter of YBCO, where $\Delta_d\gg\Delta_s,\Delta_R$. There are differing estimates of the parameter Δ_s/Δ_d^* of YBCO in the literature. For example, in tunneling microscope experiments the values $\Delta_s\approx 1$ MeV and $\Delta_s/\Delta_d^*\approx 0.05$ were obtained,[19] while for a Pb/YBCO *c*-HJ a range $\Delta_s/\Delta_d^*\approx 0.3-1.1$ was found.[23]

An additional factor that influences the value of I_1 is the presence of twinning in the YBCO film. In this case the *s* component can enter the expression $\Delta(\theta)=\Delta_d\cos 2\theta+\Delta_s$ with a minus sign as well, which is a reflection of the change in sign of *s* on passage through a twin boundary in YBCO, although the sign of the *d* component remains unchanged

here.[6] Consequently, $I_{c1}=0$ in the limiting case of equal areas of the two twin domains. However, it has been shown[27] that the areas of the twinned domains can be different even when a YBCO thin film is deposited on a $SrTiO_3$ substrate, which has a cubic crystal lattice. Denoting the areas of two twin domains as $(1+\zeta)/2$ and $(1-\zeta)/2$, we find that the experimentally measured value $I_{c1}\propto\zeta$. Using the values $\Delta_s/\Delta_d^*\approx 0.3-1.1$ and $\Delta_R=1.2$ mV for $R_d(V)$ (see Fig. 3) and substituting the experimental value of I_{c1} into (6), we obtain $\zeta=0.07-0.21$, in qualitative agreement with the value $\zeta=0.14$ obtained for a YBCO film 100 nm thick.[25,27]

The maximum value $I_{c2}=-0.25$ μA for $T\approx 1.7$ K is obtained from (7) for $\overline{D}\approx 3.2\times 10^{-2}$, which strongly exceeds the value of the transparency $\overline{D}$ of the Au/YBCO barrier. This discrepancy can be explained by assuming that the transparency of the Nb/Au/YBCO c-HJ varies over the area of the junction. The transparency of a Nb/Au/YBCO c-HJ is determined by the transparency of the Au/YBCO boundary, the uniformity of which over the area of the c-HJ depends on the uniformity of the distribution of the oxygen content in the surface layer of the YBCO. The finite surface roughness of a YBCO film leads to local diffusion of oxygen from the coating contacts toward the ab planes of YBCO. This can lead to scatter in the values of ρ and l over the area of the junction, resulting in fluctuations of the value of the transparency of the Au/YBCO boundary.

It should be noted that the second harmonic of the CPR also arises in the model of $d+is$ type symmetry of the superconducting order parameter of YBCO, which was proposed in Ref. 28 ($i=\sqrt{-1}$). However, in the framework of that model a phase shift $\varphi_0=\pi/2$ between I_{c2} and I_{c1} should exist, in disagreement with the value $\varphi_0=\pi$ determined from experiment and also with the results of Ref. 6.

A possible alternative explanation of the experimentally observed CPR is the model proposed by Millis.[29] In that model one can represent the Nb/Au/YBCO c-HJ as a lattice of 0- and π-junctions connected in parallel, with a lattice constant equal to the characteristic size of a twin domain in a c-oriented YBCO film, 10 nm. Then, as was shown in Ref. 29, spontaneous currents arise in the ground state of a c-HJ, and the energy of the c-HJ is minimum for $\varphi=\pm\pi/2$. Estimates of the value of the amplitude of the second harmonic of the CPR (I_{c2m}) arising on account of this mechanism showed that $I_{c2m}/I_{c2}<0.03$.[25] Consequently, the contribution of this mechanism to the value of I_{c2} is small.

Another alternative cause for the appearance of the second harmonic in the CPR in Nb/Au/YBCO c-HJs may be the presence of the Nb/Au boundaries, which have high transparency ($\overline{D}_{\mathrm{Nb/Au}}\sim 10^{-1}$), which is reflected in the shape of the I–V characteristic (see Fig. 3). As we have said, a Nb/Au/YBCO c-HJ can be represented as a highly asymmetric double-barrier structure, in which the second harmonic of the CPR can appear.[18] On the other hand, simple estimates based on Eq. (9) of Ref. 18 show that in such a case $I_{c2}/I_{c1}\sim\overline{D}$, and consequently the amplitude of the second harmonic of the CPR is much smaller than that observed experimentally.

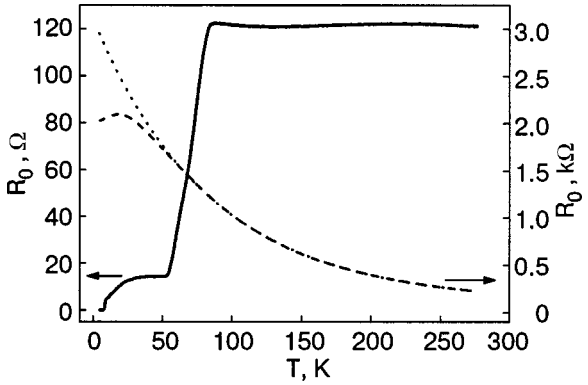

FIG. 6. Temperature dependence of the resistance R_0 of two types of inclined heterojunctions: Nb/Au/YBCO (solid curve) and Au/YBCO (dashed curve), measured at a bias current of 1 μA. The dotted curve shows the dependence $R[\mathrm{k}\Omega]=0.11+3\exp(-T[\mathrm{K}]/85)$, which is a good approximation for the experimental dependence of $R_0(T)$ of the Au/YBCO IHJ at $T>T_c=53$ K.

4. HETEROJUNCTIONS ON INCLINED FILMS (1 1 20)YBCO AND THEIR PROPERTIES

4.1. Temperature dependence of the resistance of inclined heterojunctions

Figure 6 shows the temperature dependence of the resistance R_0 measured at a current of 1 μA on inclined heterojunctions (IHJs) Au/YBCO (1 1 20) and Nb/Au/YBCO (1 1 20). It is seen that for $T\simeq 53$ K the resistance R_0 of the Au/YBCO IHJ increases exponentially with decreasing temperature, and for $T<53$ K a deviation of $R_0(T)$ from the exponential dependence is observed. In the case of the Au/YBCO IHJ one does not observe any significant change of R_0 at $T\approx T_c$, since the resistance R_N of the IHJ itself[4)] is substantially larger than the resistance of the YBCO(1 1 20) leads. This is the typical situation for Au/YBCO IHJs prepared by depositing the Au film on YBCO(1 1 20) *ex situ*. In this case the escape of oxygen atoms from the YBCO(1 1 20) surface layer decreases the transparency of the boundary. The characteristic boundary resistance r varied over wide limits, $10^{-2}-10^{-6}$ $\Omega\cdot\mathrm{cm}^2$, depending on the technique used to prepare theoretical IHJ. In particulate, for an IHJ for which the boundary between the Au and YBCO(1 1 20) was formed by depositing the Au film *ex situ*, r increased by 3–4 orders of magnitude as compared to IHJs for which the boundary between Au and YBCO(1 1 20) was formed *in situ*. Here one can speak of a decrease in $\overline{D}$ by the same factor by which r increases.

The behavior of $R_0(T)$ is completely different for $R_N \ll R_e$, which is the situation when the Au film has been deposited *in situ*. This is the case for the Nb/Au/YBCO IHJ whose $R_0(T)$ dependence is shown in Fig. 6. At $T\approx T_c=53$ K a sharp increase of R_0 is observed, due to the transition of the leads to the superconducting state. Upon further decrease of the temperature below T_c to $T_{c\mathrm{Nb}}\approx 9.2$ K the zero-bias resistance R_0 increases monotonically. The temperature at which $R_0(T)$ for the Au/YBCO IHJ deviates from the exponential dependence coincides with $T_c=53$ K.

In Au/YBCO and Nb/Au/YBCO IHJs the behavior of $R_0(T)$ for $T<T_c$ is due to the turning on of a current transport channel involving Andreev reflection as the temperature

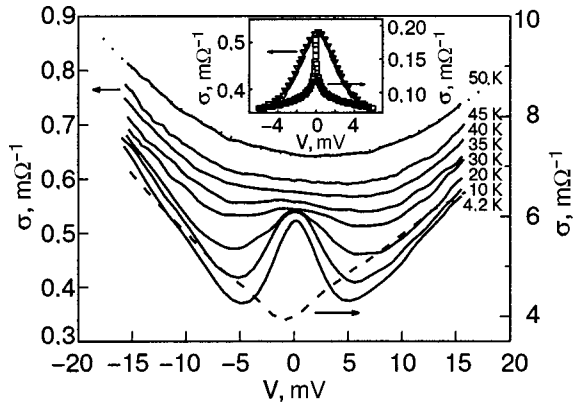

FIG. 7. Conductivity versus bias $\sigma(V)$ for an inclined Au/YBCO heterojunction at different temperatures (the solid curves from bottom to top): 4.2, 10, 20, 30, 35, 40, 45, and 50 K. The dotted curve shows the parabola approximating the dependence $\sigma(V)$ at $T=50$ K. The dashed curve corresponds to $\sigma(V)$ at $T=4.2$ K for the Au/YBCO *c*-HJ. The inset shows $\sigma(V)$ for IHJs Au/YBCO at $T=4.2$ K (inverted triangles) and Nb/Au/YBCO at $T=10$ K (squares) in the low-voltage region $|V|<6$ mV. The solid chamber is the approximation of $\sigma(V)$ for the Au/YBCO IHJ by a Lorentzian.

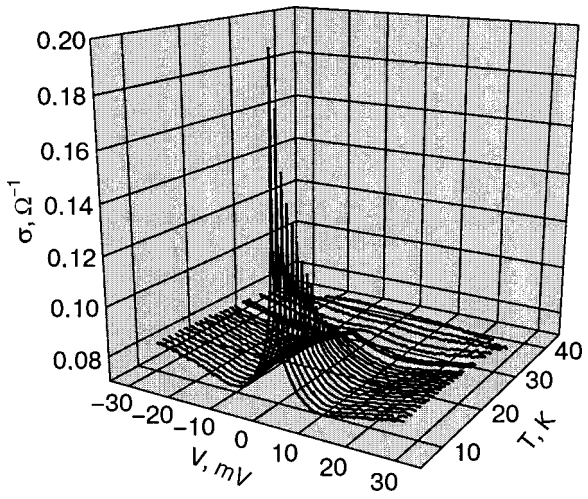

FIG. 8. $\sigma(V,T)$ for the Nb/Au/YBCO IHJ.

is lowered.[7] For IHJs on YBCO(1 1 20) films the influence of the LABSs should be manifested on the I–V characteristic in the form a conductance peak appearing at low voltages, i.e., the conductance anomaly that is observed experimentally.

4.2. Broadening of the Andreev states

Figure 7 shows the transformation of $\sigma(V)$ with decreasing temperature for a Au/YBCO IHJ. For $T>T_c$ the $\sigma(V)$ curve (the $T=50$ K curve in Fig. 7) can be approximated well by a parabola (the dashed curve in Fig. 7) in the framework of the tunneling theory of N/N' junctions with allowance for the influence of the voltage on the shape of the potential barrier.[30] For $T<T_c$ the $\sigma(V)$ curve at small V exhibits a deviation from the parabolic shape in the form of a conductance anomaly, increasing with decreasing T. The deviation of $R_0(T)$ for a Au/YBCO IHJ from the exponential growth corresponds to the onset of the conductance anomaly on the I–V characteristic. We note that the conductance anomaly is absent for the *c*-HJ Au/YBCO (dashed curve in Fig. 7).

Figure 8 shows $\sigma(V)$ for a Nb/Au/YBCO IHJ in the temperature region 9–40 K in which the conductance anomaly is most strongly expressed. We note that $\sigma(V)\approx$consts at $T=T_c$. This corresponds to the tunneling of quasiparticles through a delta-function-like barrier which is uniform over area, while for $T<T_c$ a conductance anomaly appears on the I–V characteristic of the Nb/Au/YBCO IHJ, just as for the Au/YBCO IHJ. For both types of IHJ one observes growth of the amplitude and a decrease of the half-width ΔV of the conductance anomaly as the temperature is lowered. Together with the thermal smearing of the conductance anomaly the LABS levels broaden on account of the finite lifetime of the states. For a quasiparticle with energy ε at $\varepsilon<\Delta_0$ (Δ_0 is the amplitude value of the energy gap $\Delta(\theta)=\Delta_0\cos 2\theta$ for the *d*-superconductor) one uses the following form of the density of states $N(\varepsilon,\theta)$:[8,12,31]

$$N(\varepsilon,\theta)=\frac{\pi^{-1}\Gamma^2(\theta)}{(\varepsilon-\varepsilon_b)^2+\Gamma(\theta)^2}, \tag{8}$$

where θ is the angle of incidence of the quasiparticle relative to the normal to the boundary, and ε_b describes the shift of the energy levels of the Andreev states, e.g., on account of the the flow of current along the N/d boundary. In formula (8) the level broadening is characterized by the parameter $\Gamma(\theta)\sim\hbar/\tau(\theta)$, where $\tau(\theta)$ is the lifetime of a quasiparticle in the LABS. In the general case $\Gamma(\theta)$ is determined by the tunneling of quasiparticles, $\Gamma_{\text{tunn}}(\theta)$, the diffusive scattering due to the rough surface of the YBCO film, $\Gamma_{\text{diff}}(\theta)$, umklapp processes of quasiparticle scattering with a change of the normal component of the momentum, $\Gamma_U(\theta)$, and scattering on lattice defects and impurities, Γ_{imp}:[31]

$$\Gamma(\theta)=\Gamma_{\text{tunn}}(\theta)+\Gamma_{\text{diff}}(\theta)+\Gamma_U(\theta)+\Gamma_{\text{imp}}. \tag{9}$$

If upon the formation of the LABSs the dominant contribution to their broadening comes from scattering on defects and impurities, Γ_{imp}, which is independent of the direction of the quasiparticle momentum, then, as follows from (8) and (9), the dependence of the conductance anomaly has the shape of a Lorentzian of width Γ. The inset in Fig. 7 shows the experimental dependence $\sigma(V)$ at low voltages ($V<6$ mV) for the Au/YBCO IHJ at $T=4.2$ K (inverted triangles) and the Nb/Au/YBCO IHJ at $T=10$ K (squares). The $\sigma(V)$ curve for the Au/YBCO IHJ is well approximated by a Lorentzian; consequently, it is scattering on defects and impurities that determines the half-width of the conductance anomaly in this case. It is also seen from the inset in Fig. 7 that the shape of $\sigma(V)$ for the Nb/Au/YBCO IHJ is not Lorentzian.

In the Au/YBCO IHJ the formation of the boundary was done with the vacuum broken (*ex situ*), and the (1 1 20)YBCO surface of the film was subjected to the atmosphere for about an hour prior to the deposition of Au. As a result of the interaction with the atmosphere, various impurities such as CO_2 and OH were precipitated on the surface of the YBCO film, and oxygen-deficient regions, which are lattice defects, also formed. The factors mentioned lead to the formation of a large number of scattering centers in the surface layer of the YBCO film and may give the governing contribution to the broadening of the conductance anomaly. The degree of diffuseness of the surface layer on the Au/YBCO boundary can be characterized with the aid of the parameter t/l, where t is the thickness of the disordered

layer.[2] Here $t/l=0$ corresponds to the ideal Au/YBCO (1 1 20) boundary, while $t/l=\infty$ corresponds to a completely diffuse boundary. Unfortunately, there are no data in Ref. 2 for the region $t/l>0.1$, which corresponds to the Au/YBCO IHJ under study here.

Among the LABS broadening mechanisms that depend on the direction of the momentum of the incident quasiparticles are tunneling, scattering on the YBCO surface roughness, and scattering with a change in direction of the quasiparticle momentum. With increasing transparency of the boundary the probability of escape of the quasiparticles by tunneling through the barrier increases, and that should lead to an increase of $\Gamma_{\text{tunn}}(\theta)$.[31,32] However, for the Nb/Au/YBCO IHJ the values of $\overline{D}$ are at least an order of magnitude larger than for the Au/YBCO IHJ, although ΔV at low temperatures is several times smaller for the Nb/Au/YBCO IHJ than for the Au/YBCO IHJ. For example, at $T=10$ K one has $\Delta V\approx 1$ mV for the Nb/Au/YBCO IHJ and 6.8 mV for the Au/YBCO IHJ. Thus ΔV in the IHJs falls off with increasing $\overline{D}$ and, hence, the tunneling of quasiparticles is not the governing factor for the broadening of the conductance anomaly.

The LABS broadening that leads to the non-Lorentzian shape of the conductance anomaly is apparently due to two processes: diffusive scattering due to the rough surface of the YBCO film, and umklapp processes of quasiparticle scattering with a change in the normal component of the momentum. The experimental study of the influence of each of these processes on the broadening of the conductance anomaly is difficult because of problems in determining the exact distribution of transparency over the area of the junction and over angles θ, and also of determining $\Gamma(\theta)$ for each process.

4.3. Magnetic-field dependence

When an N/d IHJ is placed in a perpendicular magnetic field a screening current arises in d, shifting the LABS levels (Doppler shift of the levels).[11] Analogously, spontaneous currents can also arise in the absence of external magnetic field if on the surface of d, e.g., when the temperature is lowered below a certain critical value T_s, a transition occurs to a mixed type of symmetry $d_{x^2-y^2}+is$ of the superconducting order parameter. In both cases this leads to splitting of the LABS levels. As a result, the peak of the conductance anomaly in an N/d IHJ is split into two peaks. In a perpendicular magnetic field H the LABS level splitting is[12]

$$\varepsilon_b=(e/c)v_F H\lambda_L \sin\theta, \tag{10}$$

where c is the speed of light in vacuum, v_F is the Fermi velocity in the ab plane of YBCO, and λ_L is the London penetration depth of the magnetic field in the c direction of YBCO. For studying a Au/YBCO IHJ in magnetic fields up to 5 T perpendicular to the plane of the substrate (making an angle of approximately 79° with the ab plane of YBCO), after subtraction of the analogous dependence for $H=0$ the presence of splitting of the conductance anomaly becomes obvious (Fig. 9). The inset in Fig. 9 shows the dependence of the splitting of the conductance anomaly on the value of the magnetic field, $\delta(H)$, in a Au/YBCO IHJ at $T=4.2$ K. In the high magnetic field region ($H>2$ T) the splitting $\delta(H)$ is practically constant and can be approximated well by the dependence $\delta(H)$ obtained in the framework of a Doppler shift model for the LABS levels owing to the generation of an additional s component of the superconducting order parameter at $T<T_s(\text{YBCO})\approx 7$ K (the solid curve in the inset of Fig. 9).[11,32] In this case the conductance anomaly should also be split at zero magnetic field, which has not been observed in experiment, even though the condition $T<T_s$ is met. It has been shown[32] that the splitting in zero magnetic field vanishes when the doping level of the d-superconductor goes from overdoping to underdoping. Apparently it is the underdoping by carriers due to the oxygen deficit that is realized in the YBCO films, as is indirectly confirmed by the low transition temperature to the superconducting state ($T_c=53$ K). In the low-magnetic-field region ($H<1$ T) the experimental data are insufficient for making a comparison of experiment with the theory.[11]

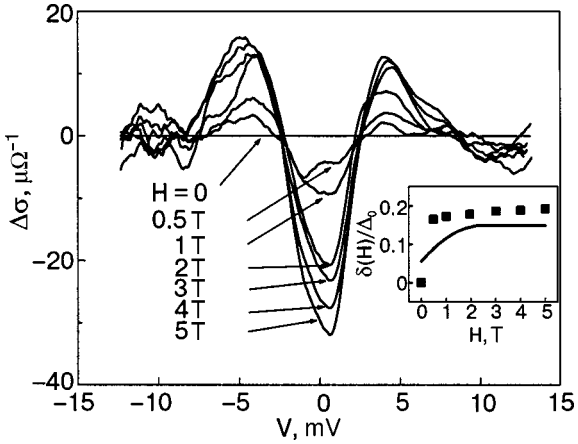

FIG. 9. $\Delta\sigma(V,H)=\sigma(V,H)-\sigma(V,0)$ at $T=4.2$ K for a Au/YBCO IHJ at various values, from 0 to 5 T, of the magnetic field applied perpendicular to the plane of the substrate. The curve for $H=0$ corresponds to a straight line passing through zero. In the inset the squares show the dependence of the splitting, calculated as half the distance between maxima of $\Delta\sigma(V,H)$ and normalized to $\Delta_0=20$ MeV, on the magnetic field strength. The solid curve corresponds to a calculation in a model in which an additional s component of the order parameter in YBCO is generated at temperatures below $T_s<7$ K, wherein $\Delta_{s-\text{YBCO}}=1.2$ meV, $\Delta_0=20$ MeV, $H_0=16$ T, and $H_c=1$ T.[12]

4.4. Influence of Andreev states on the supercurrent

The dependence of the energy of Andreev bound states on the phase difference φ of the superconducting order parameter of the electrodes forming the Josephson junction determines the supercurrent that flows through the Andreev bound states (see, e.g., Ref. 33):

$$I_s(\varphi)\propto \sum_{-\pi/2}^{\pi/2} \cos\theta_n \frac{dE_n(\theta,\varphi)}{d\varphi} f(E_n(\theta))\,d\theta, \tag{11}$$

where the summation over n goes over all the Andreev states with energies E_n, and $f(\varepsilon)$ is the Fermi distribution function. We note that for tunnel junctions made from s-superconductors ($\overline{D}\ll 1$) the energies of the Andreev states lie near the gap. For the Andreev states of a contact between an s-superconductor (Δ_R) with the (110) plane of a d-superconductor ($s/d_{(110)}$) there are also LABS levels for $\varepsilon\ll\Delta_d$:[8,33]

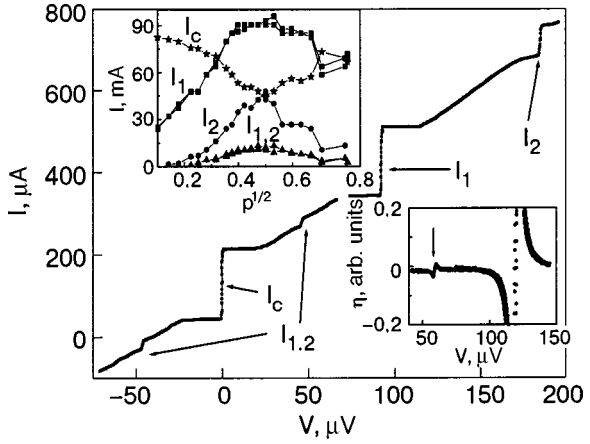

FIG. 10. I–V characteristic of a Nb/Au/YBCO IHJ of area 30×30 μm under irradiation by microwave radiation with a frequency of 46.4 GHz at $T=4.2$ K. The upper inset shows the critical current I_c and the first I_1 and second I_2 Shapiro steps as functions of the amplitude of the microwave radiation. The lower inset shows the selective detector response $\eta(V)$ obtained during irradiation by a low-power signal at $f=55.7$ GHz. The arrow indicates the subharmonic response.

$$E_n=\Delta_R\Delta_d\overline{D}\sin\varphi/[2\Delta_R+\overline{D}(\Delta_d-\Delta_R)]+O(\overline{D}^2). \quad (12)$$

It was shown in Ref. 33 that in $d/d_{(110)}$ junctions at low temperatures ($kT\ll\overline{D}\Delta_d/4\sqrt{2}$), just as in s/s junctions $I_c\propto\overline{D}$ and $I_cR_N\sim\pi\Delta_1/e$, but $I_s(\varphi)$ differs strongly from sinusoidal, $I_s(\varphi)\sim\cos\varphi$ $(0<\varphi<\pi)$ (case *a*). At higher temperatures ($\overline{D}\Delta_d/4\sqrt{2}\leqslant kT\leqslant\Delta_d/2$)$I_c\propto\overline{D}^2$, $I_cR_N\sim(\pi\Delta_d\overline{D}/4e)(\Delta_d/2kT-1)$ and $I_s(\varphi)\sim\sin2\varphi$ (case *b*). On the other hand, if $\Delta_d/2\leqslant kT\leqslant kT_c$, then $I_cR_N\approx0$.[33] Since $\overline{D}\sim10^{-4}-10^{-5}$ in the Nb/Au/YBCO iHJs studied here, we have $\overline{D}\Delta_d/4\sqrt{2}<0.01$ K, and at $T=4.2$ K case *b* is realized. For example, for a Nb/Au/YBCO IHJ with $\overline{D}\sim2.5\times10^{-5}$ one calculates $I_cR_N\approx10$ μV, which agrees in order of magnitude with the value observed in experiment. The $I_c(T)$ curve measured experimentally for the Nb/Au/YBCO IHJs falls off monotonically with increasing temperature. The nonmonotonicity of $I_c(T)$ predicted in Ref. 33 is not observed. At the same time, tunneling experiments in s/d *c*-HJs have revealed the presence of an additional *s* component of the superconducting order parameter of YBCO, with an energy gap $\Delta_{s-\mathrm{YBCO}}$. In that case the temperature dependence of the supercurrent, determined from formula (6) with allowance for the fact that, owing to the high transparency of the Nb/Au boundary and the proximity effect in the Au spacer layer, an order parameter with a critical temperature $T_c'\leqslant T_{c\mathrm{Nb}}$ can be manifested, in qualitative agreement with the experimental observations on Nb/Au/YBCO IHJs.

4.5. Phase dependence of the supercurrent of inclined Nb/Au/YBCO heterojunctions

Figure 10 shows the I–V characteristic of a 30×30 μm Nb/Au/YBCO IHJ under irradiation by monochromatic electromagnetic radiation with a frequency $f_e\approx46.4$ GHz. The I–V characteristic shows the critical current I_c, harmonic Shapiro steps I_1 and I_2, and also the first subharmonic step, with $I_{1/2}/I_1\approx0.1$ at 4.2 K.[5)] The upper inset in Fig. 10 shows the dependence of I_c, I_1, and I_2 on the normalized amplitude of the rf current for an IHJ of area 30×30 μm. The amplitudes of I_c, I_1, and I_2 oscillation with increasing amplitude of the external influence; this corresponds to a resistive model of Josephson junctions.[15] The subharmonic Shapiro steps observed experimentally on the I–V characteristic of both *c*-HJ and IHJ Nb/Au/YBCO at $V=\frac{1}{2}(hf/2e)$ are indicative of a deviation of the CPR from sinusoidal form. It should be noted that the high-amplitude irradiation of the heterojunctions under study from an external microwave source can alter the quasiparticle Fermi distribution function that appears in formula (11) for the phase dependence of the supercurrent.[34] We therefore made measurements of the selective detector response at a low amplitude of the external microwave signal relative to the value of the critical current of the Josephson junction under study, $I_{RF}\ll I_c$.

The lower inset in Fig. 10 shows the selective detector response $\eta(V)$ obtained under the influence of a low-power signal $I_{RF}\ll I_c$ with $f=55.7$ GHz. The arrow on the $\eta(V)$ curve indicates the feature at voltage $V=\frac{1}{2}(hf/2e)$, corresponding to the first subharmonic Shapiro step, the appearance of which in the given case cannot be explained by the onset of a nonequilibrium energy distribution function for the quasiparticles. For a Nb/Au/YBCO IHJ with $A=10\times10$ μm and $I_c<3$ μA we were unable to observe subharmonic Shapiro steps on the I–V characteristic, probably because of their small amplitudes.

4.6. Noise properties of inclined Nb/Au/YBCO heterojunctions

The noise properties of Nb/Au/YBCO IHJs were studied by two methods: direct measurement of the noise spectral density by a low-noise cooled amplifier working in the frequency range 1–2 GHz, and by the method of estimating the linewidth of the characteristic Josephson generation from the selective detector response to a weak external microwave signal. The I–V characteristic and the dependence of the noise power on the bias current for a Nb/Au/YBCO IHJ of area 10×10 μm are shown in Fig. 11*a*. Unlike the case of d/d contacts,[35] there is no increase in the noise on the resistive part at low values of the bias current. We note that the drop in the noise power upon the transition of the IHJ from the superconducting to the resistive state is caused by a change in the output impedance of the sample relative to the 50-Ω input impedance of the amplifier. Upon a significant increase in the bias voltage a growth of the noise spectral density $S(V)$ at the contact is observed; see Fig. 11*b*. The inset to Fig. 11*b* shows the part of the $S(V)$ curve for $|V|<9$ mV in greater detail. The dependence found is explained by growth of the shot-noise intensity $S_I=2eI$ as the current I_c through the heterojunction increases. We note that qualitatively similar $S(V)$ curves have been obtained previously[35] for d/d superconducting Josephson junctions with an averaged boundary transparency $\overline{D}\sim0.01$. The question of noise has been studied theoretically[36–38] for s/d junctions with relatively high transparency, $\overline{D}>0.1$, quite unlike the Nb/Au/YBCO IHJs studied experimentally, for which $\overline{D}\sim10^{-5}$.

It follows from Refs. 36–38 that suppression of the ex-

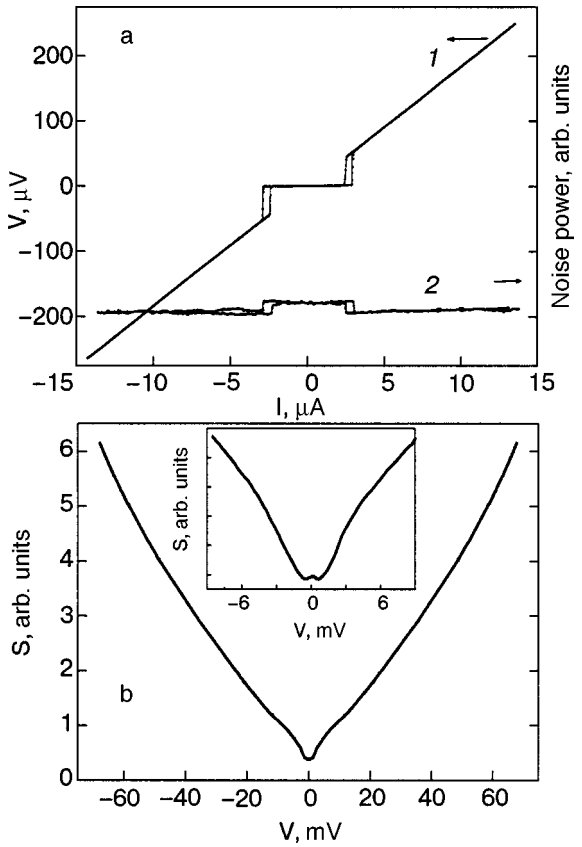

FIG. 11. I–V characteristic (*1*) and the dependence of the noise power on the bias current (*2*) for a Nb/Au/YBCO IHJ, obtained with the use of a low-noise cooled amplifier at $T=4.2$ K (*a*); dependence of the noise spectral density $S(V)$ on the voltage at $V\geqslant 50$ mV; the inset shows the part of $S(V)$ for $V<9$ mV (*b*).

cess shot noise occurs as the transparency decreases at low bias voltages for Josephson junctions with a *d*-superconductor as one or both electrodes. Most likely the absence of excess shot noise at low voltages $|V|<1$ mV in Nb/Au/YBCO IHJs can be explained by a decrease in the probability of Andreev reflection. The absence of excess noise is also shown by a second method of estimating the characteristic noise temperature of a heterojunction, which in the framework of the resistive model of Josephson junctions should be close to the physical temperature of the sample. An estimate of the linewidth Δf of the characteristic Josephson generation of a Nb/Au/YBCO IHJ based on the dependence $\eta(V)$ (the lower inset in Fig. 10) gives a value $\Delta f=4.4$ GHz, which is only 30% higher than the theoretical estimate made from the resistive model of Josephson junctions with only the contribution of the thermal fluctuations to the line broadening of the characteristic Josephson generation taken into accout. This fact again confirms the absence of excess noise in the Nb/Au/YBCO IHJs at low bias voltages.

CONCLUSION

We have investigated experimentally the superconducting and quasiparticle electron transport in thin-film HTSC heterojunctions Au/YBCO and Nb/Au/YBCO on the basis of *c*- and (1 1 20)-oriented YBCO films on (001)$SrTiO_3$ and (7 10 2)$NdGaO_3$ substrates, respectively. Studies of the dependence of the supercurrent on the phase difference of the superconducting electrodes revealed a deviation from sinusoidal form for both types of Nb/Au/YBCO heterojunctions.

A conductance peak on the I–V characteristics of the Au/(1 1 20)YBCO and Nb/Au/(1 1 20)YBCO at low voltages was found and investigated; this is the conductance anomaly due to multiple Andreev reflection in the junctions from superconductors with a $d_{x^2-y^2}$ type of order-parameter symmetry. The Lorentzian shape and the $\propto 1/T$ temperature dependence of the amplitude of the conductance anomaly in Au/YBCO heterojunctions indicate that its broadening is due to quasiparticle scattering on impurities and lattice defects, which is independent of the direction of the quasiparticle momentum, in the YBCO near the boundary. We have investigated the shot and thermal noise in Nb/Au/(1 1 20)YBCO heterojunctions, but we observed no excess noise due to the effect of Andreev reflection.

*E-mail: gena@hitech.cplire.ru

[1)] In the presence of the order-parameter suppression near the boundary in N/d junctions, bound states can also form at finite energies.[8]

[2)] X-ray diffraction experiments on (1 1 20)YBCO films have shown that such films are single-domain and have a single twin complex,[13] unlike, for example, YBCO films on (110)$SrTiO_3$ and (120)NGO substrates.[12]

[3)] Formula (2) is valid in the case of a spherical Fermi surface of the materials in contact. We note that even in the absence of an insulating layer the transparency $D\ll 1$ for the case of a large mismatch of the Fermi velocities of the metals in contact.

[4)] For the Nb/Au/YBCO IHJ one has $R_N\equiv R_0(T_c)$, while for the Au/YBCO IHJ the value of R_N was determined from the I–V characteristic as the maximum value of the resistance at 4.2 K. The low values of T_c for the Nb/Au/YBCO IHJ ($T_c\approx 53$ K) are apparently due to the escape of oxygen from the open *ab* planes of the YBCO(1 1 20) films during preparation of the samples.

[5)] We note that, as in the case of the Nb/Au/YBCO *c*-HJ, at low amplitudes of the external influence the first Shapiro step is symmetric with respect to the autonomous I–V characteristic; this attests to the coherence of the Josephson generation in autonomous junctions.[26]

[1] C. C. Tsuei and J. R. Kirtley, Rev. Mod. Phys. **72**, 969 (2000).
[2] Y. Tanaka, Phys. Rev. Lett. **72**, 3871 (1994); Y. Tanaka and S. Kashiwaya, Phys. Rev. B **53**, R11957 (1996); Yu. S. Barash, A. A. Svidzinsky, and H. Burkhardt, *ibid.* **55**, 15282 (1997).
[3] E. Il'ichev, V. Zakosarenko, R. P. J. Ijsselsteijn, V. Schultze, H.-G. Meyer, H. E. Hoenig, H. Hilgenkamp, and J. Mannhart, Phys. Rev. Lett. **81**, 894 (1998).
[4] H. Akoh, C. Camerlingo, and S. Takada, Appl. Phys. Lett. **56**, 1487 (1990); A. G. Sun, D. A. Gajewski, M. B. Maple, and R. C. Dynes, Phys. Rev. Lett. **72**, 2267 (1994); A. S. Katz, A. G. Sun, K. Char, and R. C. Dynes, Appl. Phys. Lett. **66**, 105 (1995).
[5] R. Kleiner, A. S. Katz, A. G. Sun, R. Summer, D. A. Gajewski, S. H. Han, S. I. Woods, E. Dantsker, B. Chen, K. Char, M. B. Maple, R. C. Dynes, and John Clarke, Phys. Rev. Lett. **76**, 2161 (1996).
[6] K. A. Kouznetsov, A. G. Sun, B. Chen, A. S. Katz, S. R. Bahcall, John Clarke, R. C. Dynes, D. A. Gajewski, S. H. Han, M. B. Maple, J. Giapintzakis, J.-T. Kim, and D. M. Ginsberg, Phys. Rev. Lett. **79**, 3050 (1997).
[7] A. F. Andreev, Zh. Éksp. Teor. Fiz. **46**, 1823 (1964) [Sov. Phys. JETP **19**, 1228 (1964)]; Zh. Éksp. Teor. Fiz. **49**, 655 (1965) [Sov. Phys. JETP **22**, 455 (1966)].
[8] T. Löfwander, V. S. Shumeiko, and G. Wendin, Semicond. Sci. Technol. **14**, R53 (2001).
[9] J. Lesueur, L. H. Greene, W. L. Feldmann, and A. Inam, Physica C **191**, 325 (1992).
[10] Yu. S. Barash, A. A. Svidzinsky, and H. Burkhardt, Phys. Rev. B **55**, 15282 (1997).
[11] M. Fogelström, D. Rainer, and J. A. Sauls, Phys. Rev. Lett. **79**, 281 (1997).
[12] M. Aprili, E. Badica, and L. H. Greene, Phys. Rev. Lett. **83**, 4630 (1999); R. Krupke and G. Deutscher, *ibid.* **83**, 4634 (1999); J. Lesueur, X. Grison, M. Aprili, and T. Kontos, J. Low Temp. Phys. **117**, 539 (1999).

[13] I. K. Bdikin, P. B. Mozhaev, G. A. Ovsyannikov, F. V. Komissinskiĭ, I. M. Kotelyanskiĭ, and E. I. Raksha, Fiz. Tverd. Tela (St. Petersburg) **43**, 1548 (2001) [Phys. Solid State **43**, 1161 (2001)].
[14] E. Il'ichev, V. Zakosarenko, L. Fritzsch, R. Stolz, H. E. Hoenig, H.-G. Meyer, M. Gotz, A. B. Zorin, V. V. Khanin, A. B. Pavolotsky, and J. Niemeyer, Rev. Sci. Instrum. **72**, 1882 (2001).
[15] K. K. Likharev and B. T. Ulrich, *Systems with Josephson Junctions: Basic Theory* [in Russian], MGU, Moscow (1978).
[16] M. Yu. Kupriyanov and K. K. Likharev, IEEE Trans. Magn. **MAG-27**, 2460 (1991).
[17] F. V. Komissinskiĭ, G. A. Ovsyannikov, Yu. V. Kislinskiĭ, I. M. Kotelyanskiĭ, and Z. G. Ivanov, Zh. Éksp. Teor. Fiz. **122**, 1247 (2002) [JETP **95**, 1074 (2002)].
[18] M. Yu. Kupriyanov, A. Brinkman, A. A. Golubov, M. Siegel, and H. Rogalla, Physica C **326–327**, 16 (1999).
[19] J. Y. T. Wei, N.-C. Yeh, D. F. Garrigus, and M. Strasik, Phys. Rev. Lett. **81**, 2542 (1998).
[20] V. Zaĭtsev, Zh. Éksp. Teor. Fiz. **86**, 1742 (1984) [Sov. Phys. JETP **59**, 1015 (1984)].
[21] M. Yu. Kuprianov and V. F. Lukichev, Zh. Éksp. Teor. Fiz. **94**(6), 139 (1988) [Sov. Phys. JETP **67**, 1164 (1988)].
[22] A. V. Zaĭtsev, JETP Lett. **51**, 41 (1990); A. F. Volkov, A. V. Zaitsev, and T. M Klapwijk, Physica C **210**, 21 (1993).
[23] G. Sun, A. Truscott, A. S. Katz, R. C. Dynes, B. W. Veal, and C. Gu, Phys. Rev. B **54**, 6734 (1996).
[24] H. J. H. Smilde, H. Hilgenkamp, G. J. Gerritsma, D. H. A. Blank, and H. Rogalla, IEEE Trans. Appl. Supercond. **11(2)**, 501 (2001).
[25] F. V. Komissinskiĭ, G. A. Ovsyannikov, E. Il'ichev, and Z. Ivanov, JETP Lett. **73**, 361 (2001); P. V. Komissinski, E. Il'ichev, G. A. Ovsyannikov, S. A. Kovtonyuk, M. Grajcar, R. Hlubina, Z. Ivanov, Y. Tanaka, N. Yoshida, and S. Kashiwaya, Europhys. Lett. **57**, 585 (2002).
[26] V. N Gubankov, V. P. Koshelets, and G. A. Ovsyannikov, Zh. Éksp. Teor. Fiz. **71**, 348 (1976) [Sov. Phys. JETP **44**, 181 (1976)].
[27] N. Didier, C. Dubourdieu, A. Rosova, B. Chenevier, V. Galindo, and O. Thomas, J. Alloys Compd. **251**, 322 (1997).
[28] M. Sigrist, K. Kuboki, P. A. Lee, A. J. Millis, and T. M. Rice, Phys. Rev. B **53**, 2835 (1996); R. Haslinger and R. Joynt, J. Phys.: Condens. Matter **12**, 8179 (2000).
[29] J. Millis, Phys. Rev. B **49**, 15408 (1994).
[30] J. G. Simmons, J. Appl. Phys. **34**, 1793 (1963).
[31] M. B. Walker and P. Pairor, Phys. Rev. B **60**, 10395 (1999); **59**, 1421 (1999); M. B. Walker and P. Pairor, Physica C **341–348**, 1523 (2000).
[32] G. Deutscher, Y. Dagan, A. Kohen, and R. Krupke, Physica C **341–348**, 1629 (2000); Y. Dagan and G. Deutscher, Phys. Rev. Lett. **87**, 177004 (2001).
[33] R. A. Riedel and P. F. Bagwell, Phys. Rev. B **57**, 6084 (1998).
[34] A. A. Golubov, M. Yu. Kupriyanov, and E. Il'ichev, Rev. Mod. Phys. **76**, 411 (2004).
[35] K. Y. Constantinian, G. A. Ovsyannikov, I. V. Borisenko, J. Mygind, and N. F. Pedersen, Physica C **367**, 276 (2002).
[36] Y. Tanaka, T. Asai, N. Yoshida, J. Inoue, and S. Kashiwaya, Phys. Rev. B **61**, R11902 (2000).
[37] T. Löfwander, V. S. Shumeiko, and G. Wendin, Physica C **377**, 86 (2002).
[38] J. C. Cuevas and M. Fogelström, Phys. Rev. B **64**, 104502 (2001); Phys. Rev. Lett. **89**, 227003 (2002).

Translated by Steve Torstveit